

Editorial Manager(tm) for Journal of Pharmacy and Pharmacology  
Manuscript Draft

Manuscript Number: JPP-D-09-00545R1

Title: Enhanced skin permeation and hydration by magnetic field array: preliminary in vitro and in vivo assessment

Article Type: Special Issue

Corresponding Author: Dr Heather Benson,

Corresponding Author's Institution: Western Australian Bimedical Research Institute

First Author: Heather Benson

Order of Authors: Heather Benson; Gayathri Krishnan; Jeffrey Edwards; Yih Miin Liew; Vincent P Wallace

**Enhanced skin permeation and hydration by magnetic field array: preliminary  
in vitro and in vivo assessment**

**Heather A E Benson<sup>1</sup>, Gayathri Krishnan<sup>1</sup>, Jeffrey Edwards<sup>2</sup>, Yih Miin Liew<sup>3</sup>,  
Vincent P. Wallace<sup>3</sup>**

<sup>1</sup>Curtin Health Innovation Research Institute, School of Pharmacy, Curtin University,  
Perth, WA; <sup>2</sup>OBJ Ltd, Perth, WA; <sup>3</sup>Optical+Biomedical Engineering Laboratory,  
School of Electrical, Electronic and Computer Engineering, University of Western  
Australia, Perth, WA

*Correspondence:*

Dr Heather Benson

School of Pharmacy

Curtin University

GPO Box U1987

Perth, WA 6845

Australia

Email: [h.benson@curtin.edu.au](mailto:h.benson@curtin.edu.au)

Tel: +61 8 9266 2338

Fax: +61 8 9266 2769

## ABSTRACT

Objectives: To determine the effect of a magnetic film array technology on the skin permeation of urea.

Methods: 5% urea gel was applied to human epidermal membrane in vitro and human skin in vivo. Application of gel with magnetic film array and plastic occlusive film was compared to application of gel with a plastic occlusive film and **non-magnetic** film. In vitro epidermal penetration was determined using a Franz-type diffusion system. In vivo permeation and changes in epidermal properties were visualized by optical coherence tomography (OCT).

Key findings: The mean cumulative permeation of urea over 2 h for magnetic film array application was  $89.54 \pm 7.34 \mu\text{g}/\text{cm}^2$  as compared to  $20.83 \pm 2.02 \mu\text{g}/\text{cm}^2$  for passive occluded application (mean $\pm$ sem, n=9/8), representing greater than 4-fold increase over the 2 h application time period. **Administration of urea with the magnetic film array resulted in the lag time being reduced from  $40.58 \pm 3.98$  to  $21.13 \pm 6.27$  min ( $p < 0.02$ ), whilst steady state flux increased from  $0.24 \pm 0.03$  to  $0.75 \pm 0.06 \mu\text{g}/\text{cm}^2 \cdot \text{min}$  ( $p < 0.0001$ ). Under active occlusion, the relative change in epidermal thickness as determined by OCT increased by 16% and 11% at 30 and 60 min respectively.**

Conclusions: Administration with a novel magnetic film array technology provided enhanced skin penetration of urea and increased epidermal hydration when compared to administration under an occlusive film only.

## INTRODUCTION

Dry skin is the most common dermatological problem and is widely treated by topical application of moisturizers of many different compositions. Rawlings and Matts have provided excellent reviews on the role of water in the skin, dry skin and moisturisation (Rawlings et al 1994; Rawlings 2003; Rawlings & Matts 2005). Water content in and water loss from the stratum corneum play important roles in the hydration of the outer stratum corneum layers to maintain skin flexibility, and in providing sufficient water to facilitate enzyme reactions involved in stratum corneum maturation, corneodesmolysis and desquamation (Harding et al 2000). A complex mixture of low-molecular-weight, water-soluble compounds known as Natural Moisturising Factors is present in the stratum corneum to assist in moisture retention (Rawlings & Harding 2004).

Dry skin can be induced by a number of factors including: low environmental temperature and humidity; abrupt changes in conditions associated with modern indoor-climate controlled environments; soap washing causing loss of lipid and **natural moisturizing factors** from the stratum corneum; ageing and genetics (Rawlings & Matts 2008). Blank demonstrated that stratum corneum containing less than 10% water content is brittle (Blank 1952). If untreated a “dry skin cycle” is established which will lead to scaly skin with increased hardness and brittleness (Rawlings & Matts 2005). This occurs because the superficial dehydration of the stratum corneum induces release of inflammatory mediators, hyperproliferation and disruption of epidermal differentiation. However the “dry skin cycle” can be reversed by intervention with suitable moisturizing agents.

Humectants, occlusives and emollients are the most commonly used moisturizer components for management of dry skin (Rawlings et al 2004). Other moisturizing agents include bilayer-forming lipids including ceramides and phospholipids, hydroxyacids and agents that induce epidermal differentiation and lipogenesis, such as ligands for the peroxisomal proliferator-activated receptor (e.g. linoleic and other long chain fatty acid), niacinamide and vitamin C. Rawlings and Matts recently reviewed the range of moisturizers, their properties and mechanisms of action (Rawlings & Matts 2008).

Urea has been used as a humectant in moisturizing creams since 1943 (Rattner 1943) and is a natural component of the stratum corneum **natural moisturizing factors**.

Moisturizers containing urea have been reported to improve stratum corneum barrier function, reduce trans epidermal water loss, increase skin capacitance and reduce irritation (Loden 1996; Buraczewska et al 2007). Occlusive formulations such as petroleum jelly, oils and occlusive dressings act as an occlusive film on the skin surface to reduce **transepidermal water loss** and thereby hydrate the skin. Many moisturizers contain combinations of agents to optimize the hydrating effect of the product on the skin.

In the current study the influence of an un-powered magnetic film array on the permeation of urea into and through the epidermis was evaluated in vitro and the consequent hydration effect determined in vivo. In vitro permeation of urea through human epidermis was evaluated in a Franz cell diffusion system using standard protocols. In vivo determination of the hydration effects of the administered urea was

determined by optical coherence tomography (OCT) in human volunteers. Urea was administered as a simple measured dose of gel with occlusion film (control) or with occlusion film with the additional magnetic film array placed externally to the occlusive (active).

## **MATERIALS AND METHODS**

### **Materials**

All the chemicals and reagents listed below were used as supplied: Urea gel was supplied as a 5% w/w urea in VersaBase Gel (PCCA, Huston, TX) as supplied from Compounding on Oxford, Perth, W.A.; phosphate buffered saline solution pH 7.4 (PBS) was prepared according to the United States Pharmacopoeia. P-dimethylaminobenzaldehyde (DMAB) was purchased from BDH Laboratory Chemicals Group, Poole, England. Ethanol was obtained from CSR Distilleries Group, Australia and concentrated sulphuric acid from Lab Scan Asia Co Ltd, Bangkok, Thailand. **Passive occlusive material used for in vitro and in vivo consisted of a polymer film of similar thickness and cut to the same dimensions as the active magnetic polymer material. In addition, all in vitro cells and in vivo sites were further occluded with Parafilm M polymer film.**

Magnetic **film** array material consisted of 35 mm x 35 mm sections of un-powered flexible array matrix (ETP Type 008), a proprietary enhanced transdermal delivery array film developed by OBJ Limited, Perth, Western Australia. The magnetic film array (ETP Type 008) is a thin flexible polymer matrix containing multiple magnetic elements arranged to produce complex 3-dimensional magnetic gradients. **The**

material has a peak magnetic field strength of 40 mT. However the arrangement and distribution of alternating poles across the surface of the material results in a total magnetic gradient of 2 T/m<sup>2</sup>.

### **Spectroscopic Analysis**

Urea quantification was based on the analytical method of Knorst et al (Knorst et al 1997): a modified derivatisation by *p*-dimethylaminobenzaldehyde (DMAB) into a coloured compound. Derivatisation of urea in skin diffusion samples employed equal volumes of sample solution and the DMAB reagent (4% w/v) prepared with conc. sulphuric acid (4% v/v) in alcohol (95%). In this case 200µL of the urea sample was mixed with 200µL of the DMAB reagent. After 10 min the absorbance of the coloured derivatised solution was measured at 420 nm using a UVmini-1240 UV-Vis spectrophotometer (Shimadzu Scientific Instruments, NSW, Australia) against an appropriate reagent blank (receptor solution processed as for skin permeation receptor solution samples).

### **In vitro Skin Diffusion Studies**

#### ***Preparation of Epidermal Membrane***

Epidermal membranes were obtained from human skin sourced from Perth hospitals (abdominal region following abdominoplasty surgery; three female donors 50 yrs, 39 yrs and 44 yrs) with ethics approval from the Human Research Ethics Committee of Curtin University. Epidermal membranes were obtained by the heat separation method (Kligman & Christophers 1963). Briefly, the subcutaneous tissue was removed by dissection then full thickness human skin was immersed in water at 60°C for 1 min. The epidermal membrane was teased off the dermis, placed onto

aluminium foil with stratum corneum facing upward, air dried for 15 min and then stored at  $-20^{\circ}\text{C}$  (for not more than 2 months) until required.

### *In Vitro Diffusion studies*

In vitro diffusion studies across human epidermis were performed using Pyrex glass Franz-type diffusion cells (enabling permeation across epidermal membranes of cross sectional area  $1.18\text{ cm}^2$ ); receptor volume approximately 3.5 mL. The membrane was placed between the donor and receptor compartment of the cell and allowed to equilibrate for 1 h with PBS in the receptor compartment that was stirred continuously with a magnetic stirrer. PBS (1 mL) was placed in the donor and receptor compartments of the cell which was placed in a water bath maintained at  $37\pm 0.5^{\circ}\text{C}$ . Epidermal membrane integrity was then determined by visual inspection over a bright light and electrical resistance ( $\text{k}\Omega$ ), capacitance ( $\text{nF}$ ) and impedance ( $\text{k}\Omega$ ) measurements using a digital portable LCR meter (TH2821/A/B, Changzhou Tonghui Electronic Co., Ltd, China). The measurements were taken by immersing the stainless steel probe lead tips, one each in the donor and receptor compartments (Fasano et al 2002). Membranes exhibiting an electrical resistance less than  $20\text{ k}\Omega$  were rejected from the study. The diffusion cells were emptied, receptor compartments refilled with fresh preheated PBS at  $37\pm 0.5^{\circ}\text{C}$ . Urea gel (0.5 g) was placed in the donor compartment. Sections of magnetic film array were cut to a size suitable for insertion into the donor compartment of the Franz type cell and suspended above and exterior to the gel (Figure 1), whilst passive cells had **non-magnetic polymer film of similar dimensions placed above the gel. All cells were also occluded by sealing the top of the donor compartment of the cell with Parafilm.** Aliquots from the receptor phase were withdrawn from the sampling arm and replaced with fresh pre-heated (at  $37^{\circ}\text{C}$ )

PBS over a 2 h period. The total urea content permeating the epidermal membrane to the receptor solution samples obtained from individual experiments was determined by spectroscopic analysis. At time 2 h the donor and receptor fluids were recovered, the cell disassembled and the skin epidermal membrane examined for obvious tears (any cells with torn membranes were rejected). Experiments were repeated 9 times for magnetic film array enhanced (active) and 8 times for passive (control) diffusion experiments. The cumulative amount of urea permeating through the epidermis to the receptor compartment ( $\mu\text{g}/\text{cm}^2$ ) was plotted as a function of time (h) and the **steady state flux ( $\mu\text{g}/\text{cm}^2\cdot\text{h}$ ), permeability coefficient (cm/min) and lag time (min)**.

### **Statistical analysis**

**Magnetic film application and passive application were analysed using a linear mixed effects model. Data were transformed using the square-root of the measures to stabilise the variance. The within-cell correlation over time was accommodated using a first-order autoregressive correlation structure. Post hoc comparisons between conditions at each time point were evaluated using the Mann Whitney U test.**

**Permeation parameters were calculated from the data: steady state flux, permeability coefficient, lag time and cumulative amount of urea permeated at 2 h. Comparison of the parameters obtained for active and control administration were compared by unpaired t tests.**

### **In vivo hydration: Optical Coherence Tomography assessments**

**Direct measurement of penetration of urea into the skin in vivo is difficult thus OCT was utilised to measure the physical changes in the skin properties. Over the past decade OCT has emerged as a high-resolution optical diagnostic imaging modality**

widely used in ophthalmology (Choma et al 2002; Srinivasan et al 2007) and dermatology (Steiner et al 2003; Pierce et al 2004; Gambichler et al 2005). Although the spatial resolution (typically 5-20 microns) of OCT is not as good as that of histology, it enables non-invasive, *in vivo* imaging of the internal tissue microstructures. This resolution is much higher than most of the current clinical diagnostic technologies such as X-ray, computed tomography (CT) or magnetic resonance imaging (MRI). In addition, unlike X-ray and CT, OCT does not use ionising radiation, instead using light waves in the near infrared. While this significantly reduces the penetration depth to a few millimetres (approximately 3 mm) due to the optical scattering of tissue, it is sufficient to reveal images of the stratum corneum, epidermis, upper dermis, hair follicles as well as sweat glands, where most skin pathologies and conditions occur, including skin cancers (Welzel 2001; Steiner et al 2003; Gambichler et al 2005; Salvini et al 2008). Crowther et al recently demonstrated a strong, positive correlation in measurement of stratum corneum thickness between OCT and confocal Raman spectroscopy, with the latter technology offering higher resolution for thinner stratum corneum sites ( $\approx < 15 \mu\text{m}$ ) (Crowther et al 2008).

The operation of OCT is based on interference of light from a low coherence broadband light source. The working principle is analogous to ultrasound imaging (Gambichler et al 2005; Mogensen et al 2008), being based on the reflection of signal from the tissue but utilising light rather than acoustic waves. Unlike ultrasound, no direct tissue coupling is required for OCT imaging. As the tissue sample consists of different types of cells, organelles and microstructures, each with different reflective index, the incoming light beams are reflected and backscattered from different

boundaries within the tissue. Thus OCT is an important tool in monitoring of transdermal delivery of drugs that alter the skin structure.

OCT measurements were carried out using a commercial swept-source FD-OCT system (Thorlabs, Newton, NJ, USA). This system comprised a broadband, high-speed frequency swept laser and a fibre-based Michelson interferometer with a balanced detection scheme to perform depth profiling and 3D image reconstruction at video rates. The system had a handheld probe to enable in vivo scanning of the skin. The light source had a centre wavelength of 1325 nm and a full width at half maximum bandwidth of 100 nm. The average output power to the skin was 10 mW with the maximum axial scan rate of 16 kHz. Axial resolution was 12  $\mu\text{m}$  and transverse resolution was 15  $\mu\text{m}$ . Maximum imaging depth was 3 mm with a maximum imaging width of 10 mm. The scanning process involved axial and transverse scanning of the tissue sample. An axial or depth scan (A-scan) was obtained by translating the reference arm length, resulting in localized interference fringes with amplitudes related to sample reflectivity (Gambichler et al 2005). Adjacent A-scans were combined to produce B-scans (i.e. two-dimensional image), which depict the tissue's cross-sectional subsurface structures.

The study was conducted on a human volunteer (male, 55 years old) with a healthy skin type under ethics approval from the UWA. The OCT measurements were carried on two regions of skin. The first region on the inside right forearm had 5% urea gel topically applied in conjunction with occlusive Parafilm with the addition of an external ETP Type 008 (active). The second region in a similar position on the left arm, had the same amount of 5% urea gel applied and then occluded using Parafilm

and a passive polymer sheet of the same dimensions as the ETP Type 008. OCT images were acquired at 0, 30 and 60 min in triplicate. Four sites were measured from each region resulting in 72 images which were used to determine changes in epidermal thickness in response to penetration of the active ingredient, urea. The epidermal thickness was calculated from OCT images by boundary differentiated pixel counts of the region encompassed by the stratum corneum and dermal/epidermal boundary from each image. This was then coloured using a primary fill and the thickness averaged over 5 mm widths across the image (Figure 2). The average thickness was calculated for each site at each time point and the percentage increase in thickness calculated for times 30 and 60 min relative to time 0. The error on the thickness measurement is 10-15  $\mu\text{m}$ .

## **RESULTS**

### **Urea analysis**

Spectrophotometric analysis was carried out for quantitative analysis of urea that permeated the skin. Upon derivatisation with 4% DMAB reagent a coloured derivatised compound was formed in the presence of urea. All calibration curves of urea standards showed good linearity in the concentration range of 7.8-125  $\mu\text{g/mL}$  ( $r^2 = 0.99$ ;  $n=5$ ). The limit of detection (LOD) and limit of quantitation (LOQ) of the assay were 0.83 and 2.5  $\mu\text{g/mL}$  respectively.

### **In vitro skin diffusion study**

The in vitro permeation profiles of urea across human epidermis are presented in Figure 3 and permeation parameters are given in Table 1. The results were compiled

from 9 active cells (occlusion plus magnetic film) and 8 control cells (occlusion plus control film). A comparison of the cumulative amount of urea penetrating the epidermis to the receptor solution versus time was plotted for passive and magnetic array enhanced applications (Figure 3). A linear mixed effects model analysis showed a significant difference between groups ( $F_{1,15} = 19.92$ ;  $p = 0.0005$ ), a significant difference over time ( $F_{1,134} = 156.45$ ;  $p < 0.0001$ ) and a significant group \* time interaction ( $F_{1,134} = 23.02$ ;  $p < 0.0001$ ). There was a significant difference between groups at all time points ( $p < 0.02$ ). Mann Whitney U values for each comparison are included in Table 2.

There was a significant increase in the mean cumulative permeation of urea over 2 h for ETP application was ( $89.54 \pm 7.34 \mu\text{g}/\text{cm}^2$ ) as compared to passive occluded application ( $20.83 \pm 2.02 \mu\text{g}/\text{cm}^2$ ; mean  $\pm$  sem;  $p < 0.0001$  unpaired t test). All permeation parameters were significantly enhanced by magnetic application (based on unpaired t tests). The lag time was reduced from  $40.58 \pm 3.98$  to  $21.13 \pm 6.27$  min ( $p < 0.02$ ), whilst steady state flux increased from  $0.24 \pm 0.03$  to  $0.75 \pm 0.06 \mu\text{g}/\text{cm}^2 \cdot \text{min}$  ( $p < 0.0001$ ) by administration of urea with the magnetic film array (Table 1).

### **In vivo hydration: Optical Coherence Tomography assessments**

Examples of OCT images are provided in Figure 2. Over all measurements, OCT showed that 5% urea gel under passive occlusion increased the relative epidermal thickness by 3% and 6% at time points 30 and 60 minutes respectively compared with time 0. Under active occlusion, the relative change in epidermal thickness increased by 16% and 11% at 30 and 60 min respectively. These results are displayed in Figure

4; the errors of the relative change were calculated from the error in measuring the epidermal thickness. Thirty minutes after topical application of the urea gel the OCT measurements revealed an over 5-fold increase in epidermal thickness using the active ETP compared to passive occlusion. The affect was less marked at 60 minutes but there was still an almost 2-fold difference in the relative epidermal thickness comparing the active and passive occlusion.

## DISCUSSION

A comparison of the cumulative amount of urea penetrating the epidermis to the receptor solution versus time was plotted for passive and magnetic film array applications. In all cases cells were occluded and non-magnetic polymer film of similar dimensions was used as control to ensure that any increase in urea penetration was due to the magnetic field energy in the array film and not simply the occlusive effect of magnetic film in proximity to the gel. Urea penetration was significantly increased by magnetic film array compared to passive application over the time period of the experiment ( $p < 0.001$ ). All urea permeation parameters were significantly enhanced in the presence of the magnetic field.

Direct measurement of penetration of urea into the skin in vivo is difficult thus OCT was utilised to visualise and measure the physical changes in the skin properties due to hydration. As expected, the epidermal depth was increased by hydration due to occlusion and the presence of the topically administered hydrating agent urea. OCT permitted monitoring of the time dependent effects on skin properties in response to hydration. In this study the application of 5% urea gel with occlusion increased

epidermal thickness by 3% and 6% after 30 and 60 min respectively. However when urea gel was applied with the magnetic film (ETP008) the epidermal thickness increased by 18% after 30 min and 11% at 60 min. This suggests that the magnetic field array material increases hydration due by enhancing the rate of urea permeation into the skin and confirms the in vitro epidermal penetration data obtained in the study. It appears from the OCT measurements that the changes in the epidermal properties maximize after about 30 min and then stabilize or even decrease over longer periods of time. Given the difficulty in making repeat measurements in exactly the same place (positioning accuracy equals the transverse resolution of the OCT imaging system which is 15  $\mu\text{m}$ ) this may be due to changes in tissue morphology due to skin appendages like hair follicles or sweat ducts. There is the added complication that the changes in the levels of hydration may also change the refractive index of the epidermis, here for all thickness measurements we have assumed the refractive index to be 1.4. Further studies with more subjects and multiple time points are required to fully understand the in vivo changes. This will be the subject of future investigations.

Magnetic fields have been shown to induce changes in a number of cell types including fibroblasts, endothelial cells and keratinocytes (Bassett 1989, 1993; Polk & Postow 1996). They have been reported to induce wound healing (Scardino et al 1998; Matic et al 2009) and improve chronic skin ulcers (Milgram et al 2004; Callaghan et al 2008), stimulate collagen (Ahmadian et al 2006) and bone growth (Colson et al 1988), and enhance the photodynamic effect on cancer cells (Pang et al 2001). Murthy reported enhanced skin permeation of benzoic acid, salbutamol sulphate and terbutaline sulphate by magnetophoresis, which involved the use of stationary permanent magnets (Murthy 1999; Murthy &

Hiremath 1999; Murthy & Hiremath 2001). We have previously demonstrated enhanced skin penetration of 5-amino levulinic acid, a dipeptide and naltrexone hydrochloride by a pulsed electromagnetic field (Namjoshi et al 2007; Namjoshi et al 2008; Krishnan et al 2010). In the latter study a preliminary investigation to elucidate the mechanism of magnetic enhanced delivery was undertaken by applying 10 nm gold nanoparticles to human epidermis with and without electromagnetic fields. Multiphoton microscopy with fluorescent lifetime imaging microscopy (MPM-FLIM) showed skin permeation of the nanoparticles with the pulsed electromagnetic field with no evidence of passive permeation. This suggests that the magnetic energy may induce channels within the stratum corneum of at least 10 nm in diameter. **It must be noted that these studies involved a range of different types of magnetic fields to influence skin permeation of various compounds. The precise mechanism of skin permeation enhancement may vary with the magnetic field characteristics.**

## **CONCLUSIONS**

Urea gel was applied as a moisturizer. Its penetration across human epidermis was determined in vitro and epidermal hydration effect visualized in vivo by OCT. Administration with a novel magnetic film technology provided enhanced skin penetration of urea and increased epidermal hydration when compared to administration under an occlusive film. The practical benefits of an un-powered, thin and flexible magnetic film array that is suited to fabrication as a drug patch or cosmetic mask with enhanced skin delivery warrants further investigation.

## **ACKNOWLEDGEMENTS**

The statistical advice of Peter McKinnon is acknowledged. The authors thank the surgeons and patients who provided skin for this research. GK acknowledges the scholarship provided by Curtin University (CIRTS).

## **REFERENCES**

- AHMADIAN, S., ZARCHI, S. R., BOLOURI, B. (2006) Effects of extremely-low-frequency pulsed electromagnetic fields on collagen synthesis in rat skin. *Biotechnol Appl Biochem* 43: 71-5
- BASSETT, C. A. (1989) Fundamental and practical aspects of therapeutic uses of pulsed electromagnetic fields (PEMFs). *Crit Rev Biomed Eng* 17: 451-529
- BASSETT, C. A. (1993) Beneficial effects of electromagnetic fields. *J Cell Biochem* 51: 387-93
- BLANK, I. H. (1952) Factors which influence the water content of the stratum corneum. *J Invest Dermatol* 18: 433-440
- BURACZEWSKA, I., BERNE, B., LINDBERG, M., TORMA, H., LODEN, M. (2007) Changes in skin barrier function following long-term treatment with moisturizers, a randomized controlled trial. *Br J Dermatol* 156: 492-8
- CALLAGHAN, M. J., CHANG, E. I., SEISER, N., AARABI, S., GHALI, S., KINNUCAN, E. R., SIMON, B. J., GURTNER, G. C. (2008) Pulsed electromagnetic fields accelerate normal and diabetic wound healing by increasing endogenous FGF-2 release. *Plast Reconstr Surg* 121: 130-41

- CHOMA, M. A., RAO, K., CZAJKA, M., RASHED, H., WINTER, K. P., TOTH, C. A.,  
IZATT, J. A. (2002) Real-Time OCT Imaging of the Retina. ARVO 43: 4372-  
4372
- COLSON, D. J., BROWETT, J. P., FIDDIAN, N. J., WATSON, B. (1988) Treatment of  
delayed- and non-union of fractures using pulsed electromagnetic fields. J  
Biomed Eng 10: 301-4
- CROWTHER, J. M., SIEG, A., BLENKIRON, P., MARCOTT, C., MATTS, P. J.,  
KACZVINSKY, J. R., RAWLINGS, A. V. (2008) Measuring the effects of topical  
moisturizers on changes in stratum corneum thickness, water gradients and  
hydration in vivo. Br J Dermatol 159: 567-77
- FASANO, W. J., MANNING, L. A., GREEN, J. W. (2002) Rapid integrity assessment of  
rat and human epidermal membranes for in vitro dermal regulatory testing:  
correlation of electrical resistance with tritiated water permeability. Toxicol In  
Vitro 16: 731-40
- GAMBICHLER, T., MOUSSA, G., SAND, M., SAND, D., ALTMAYER, P., HOFFMANN, K.  
(2005) Applications of optical coherence tomography in dermatology. J  
Dermatol Sci 40: 85-94
- HARDING, C. R., WATKINSON, A., RAWLINGS, A. V., SCOTT, I. R. (2000) Dry skin,  
moisturization and corneodesmolysis. Int J Cosmet Sci 22: 21-52
- KLIGMAN, A., CHRISTOPHERS, E. (1963) Preparation of isolated sheets of human  
stratum corneum. Arch Dermatol 88: 70-73
- KNORST, M. T., NEUBERT, R., WOHLRAB, W. (1997) Analytical methods for  
measuring urea in pharmaceutical formulations. J Pharm Biomed Anal 15:  
1627-32

- KRISHNAN, G., EDWARDS, J., CHEN, Y., BENSON, H. A. E. Enhanced Skin Permeation of Naltrexone by Pulsed Electromagnetic Fields in Human Skin In Vitro. *J Pharm Sci* (submitted).
- LODEN, M. (1996) Urea-containing moisturizers influence barrier properties of normal skin. *Arch Dermatol Res* 288: 103-7
- MATIC, M., LAZETIC, B., POLJACKI, M., DJURAN, V., MATIC, A., GAJINOV, Z. (2009) Influence of different types of electromagnetic fields on skin reparatory processes in experimental animals. *Lasers Med Sci* 24: 321-7
- MILGRAM, J., SHAHAR, R., LEVIN-HARRUS, T., KASS, P. (2004) The effect of short, high intensity magnetic field pulses on the healing of skin wounds in rats. *Bioelectromagnetics* 25: 271-7
- MOGENSEN, M., MORSY, H. A., THRANE, L., JEMEC, G. B. (2008) Morphology and epidermal thickness of normal skin imaged by optical coherence tomography. *Dermatology* 217: 14-20
- MURTHY, S. N. (1999) Magnetophoresis: an approach to enhance transdermal drug diffusion. *Die Pharmazie* 54: 377-379
- MURTHY, S. N., HIREMATH, S. R. (1999) Effect of magnetic field on the permeation of salbutamol sulphate. *Indian Drugs* 36: 663-4
- MURTHY, S. N., HIREMATH, S. R. (2001) Physical and chemical permeation enhancers in transdermal delivery of terbutaline sulphate. *AAPS PharmSciTech* 2: E-TN1
- NAMJOSHI, S., CACETTA, R., EDWARDS, J., BENSON, H. A. E. (2007) Liquid chromatography assay for 5-aminolevulinic acid: application to in vitro assessment of skin penetration via Dermaportation. *J Chromatogr B* 852: 49-55

- NAMJOSHI, S., CHEN, Y., EDWARDS, J., BENSON, H. A. E. (2008) Enhanced transdermal delivery of a dipeptide by dermaportation. *Biopolymers* 90: 655-662
- PANG, L., BACIU, C., TRAITCHEVA, N., BERG, H. (2001) Photodynamic effect on cancer cells influenced by electromagnetic fields. *J Photochem Photobiol B* 64: 21-6
- PIERCE, M. C., STRASSWIMMER, J., PARK, B. H., CENSE, B., DE BOER, J. F. (2004) Advances in optical coherence tomography imaging for dermatology. *J Invest Dermatol* 123: 458-63
- POLK, C., POSTOW, E. (1996) *Handbook of Biological Effects of Electromagnetic Fields*. CRC Press, Boca Raton
- RATTNER, H. (1943) Dermatologic uses of urea. *Acta Derm Venereol* 37: 155-165
- RAWLINGS, A. V. (2003) Trends in stratum corneum research and the management of dry skin conditions. *Int J Cosmet Sci* 25: 63-95
- RAWLINGS, A. V., HARDING, C. R. (2004) Moisturization and skin barrier function. *Dermatol Ther* 17 Suppl 1: 43-8
- RAWLINGS, A. V., MATTS, P. J. (2005) Stratum corneum moisturization at the molecular level: an update in relation to the dry skin cycle. *J Invest Dermatol* 124: 1099-110
- RAWLINGS, A. V., MATTS, P. J. (2008) Dry skin and moisturizers. In: Walters, K. A., MS, Roberts. (eds) *Dermatologic, Cosmeceutic and Cosmetic Development*. Informa Healthcare, New York, pp 339-371
- RAWLINGS, A. V., CANESTRARI, D. A., DOBKOWSKI, B. (2004) Moisturizer technology versus clinical performance. *Dermatol Ther* 17 Suppl 1: 49-56

- RAWLINGS, A. V., SCOTT, I. R., HARDING, C. R., BOWSER, P. A. (1994) Stratum corneum moisturization at the molecular level. *J Invest Dermatol* 103: 731-41
- SALVINI, C., MASSI, D., CAPPETTI, A., STANTE, M., CAPPUGI, P., FABBRI, P., CARLI, P. (2008) Application of optical coherence tomography in non-invasive characterization of skin vascular lesions. *Skin Res Technol* 14: 89-92
- SCARDINO, M. S., SWAIM, S. F., SARTIN, E. A., STEISS, J. E., SPANO, J. S., HOFFMAN, C. E., COOLMAN, S. L., PEPPIN, B. L. (1998) Evaluation of treatment with a pulsed electromagnetic field on wound healing, clinicopathologic variables, and central nervous system activity of dogs. *Am J Vet Res* 59: 1177-81
- SRINIVASAN, V. J., HUBER, R., GORCZYNSKA, I., FUJIMOTO, J. G., JIANG, J. Y., REISEN, P., CABLE, A. E. (2007) High-speed, high-resolution optical coherence tomography retinal imaging with a frequency-swept laser at 850 nm. *Opt Lett* 32: 361-3
- STEINER, R., KUNZI-RAPP, K., SCHARFFETTER-KOCHANEK, K. (2003) Optical Coherence Tomography: Clinical Applications in Dermatology. *Medical Laser Application* 18: 249-259
- WELZEL, J. (2001) Optical coherence tomography in dermatology: a review. *Skin Res Technol* 7: 1-9

**Table 1: In vitro skin permeation parameters for urea following administration as 5% gel with ETP verses passive occluded application (values are mean  $\pm$  sem). All measures were significantly different when compared for the two treatments ( $p < 0.05$ ; unpaired t test).**

Parameters	Treatment and Time	
	0-120 min	
	Passive	ETP
Mean cumulative permeation ( $\mu\text{g}/\text{cm}^2$ )	20.83 $\pm$ 2.02	89.54 $\pm$ 7.34
Steady state flux ( $\mu\text{g}/\text{cm}^2 \cdot \text{min}$ )	0.24 $\pm$ 0.03	0.75 $\pm$ 0.06
Lag time (min)	40.58 $\pm$ 3.98	21.13 $\pm$ 6.27
Permeability coefficient (cm/h)	2.98 $\times 10^{-5} \pm 0.23$ $\times 10^{-5}$	9.61 $\times 10^{-6} \pm 1.02$ $\times 10^{-6}$

**Table 2: In vitro skin permeation: statistical analysis of difference in urea permeation over time for magnetic versus passive administration. Mann-Whitney U analysis.**

P value	Time (min)							
	10	20	30	40	50	60	90	120
	0.021	0.021	0.006	0.006	0.002	0.001	0.000	0.000

*Figure legends*

**Figure 1: Picture of in vitro setup showing placement of ETP film**

**Figure 2: Examples of optical coherence tomography images of human skin at 60 min post application of urea gel with passive occlusion and ETP magnetic array with occlusion**

**Figure 3: Cumulative amount of urea ( $\mu\text{g}/\text{cm}^2$ ) permeating human epidermis to the receptor compartment during application of 5% urea gel with ETP008 ( $\Delta$ ) verses passive occluded ( $\circ$ ) conditions (mean  $\pm$  sem; n=9 and 8 cells respectively)**

**Figure 4: Difference in epidermal thickness at time point 30 and 60 min relative to 0 min due to administration of 5% urea gel with passive and active (ETP008) occlusion giving the percentage change (mean  $\pm$  error - calculated from the error in measuring the epidermal thickness; 72 OCT images)**

**Figure 1**  
[Click here to download high resolution image](#)

**Magnetic  
Array**

**Donor  
Formulation**

**Epidermal  
Membrane**

**Receptor  
Fluid**



## Optical Coherence Tomography Images

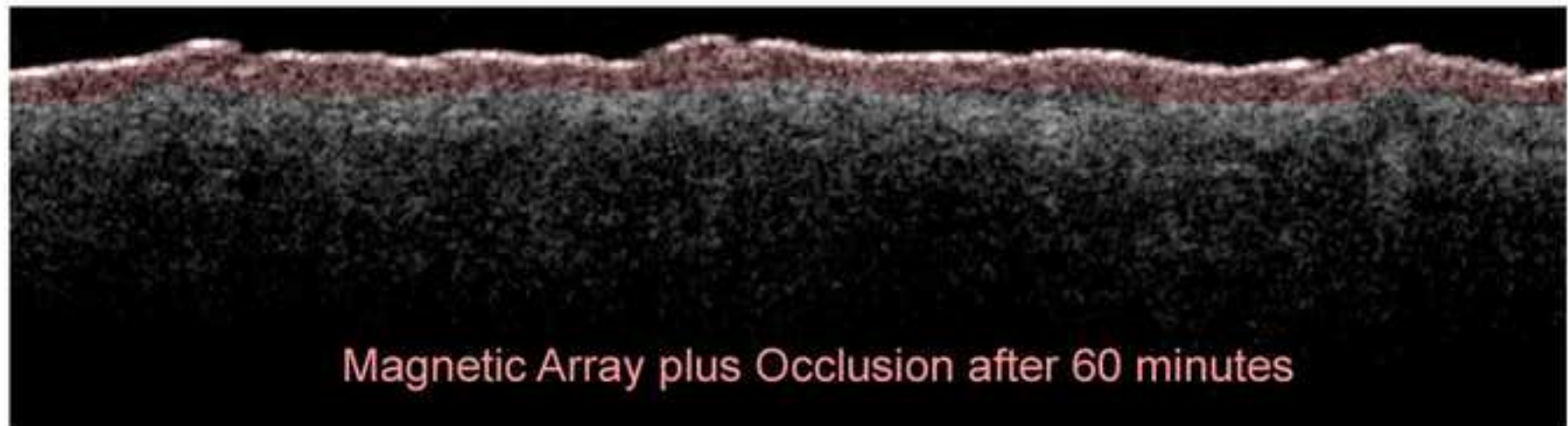
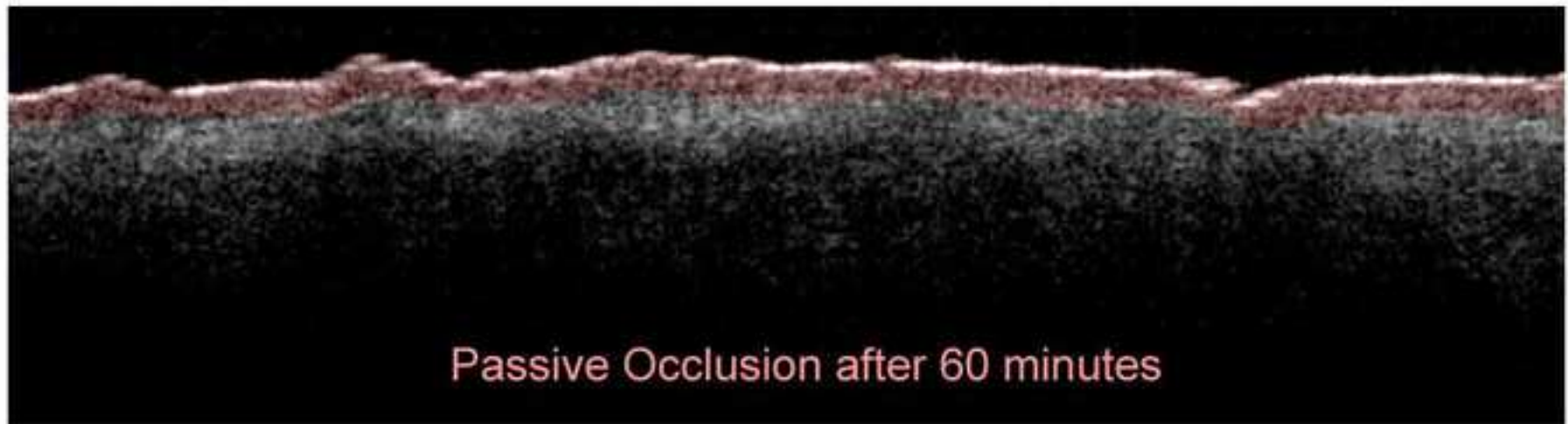


Figure 3  
[Click here to download high resolution image](#)

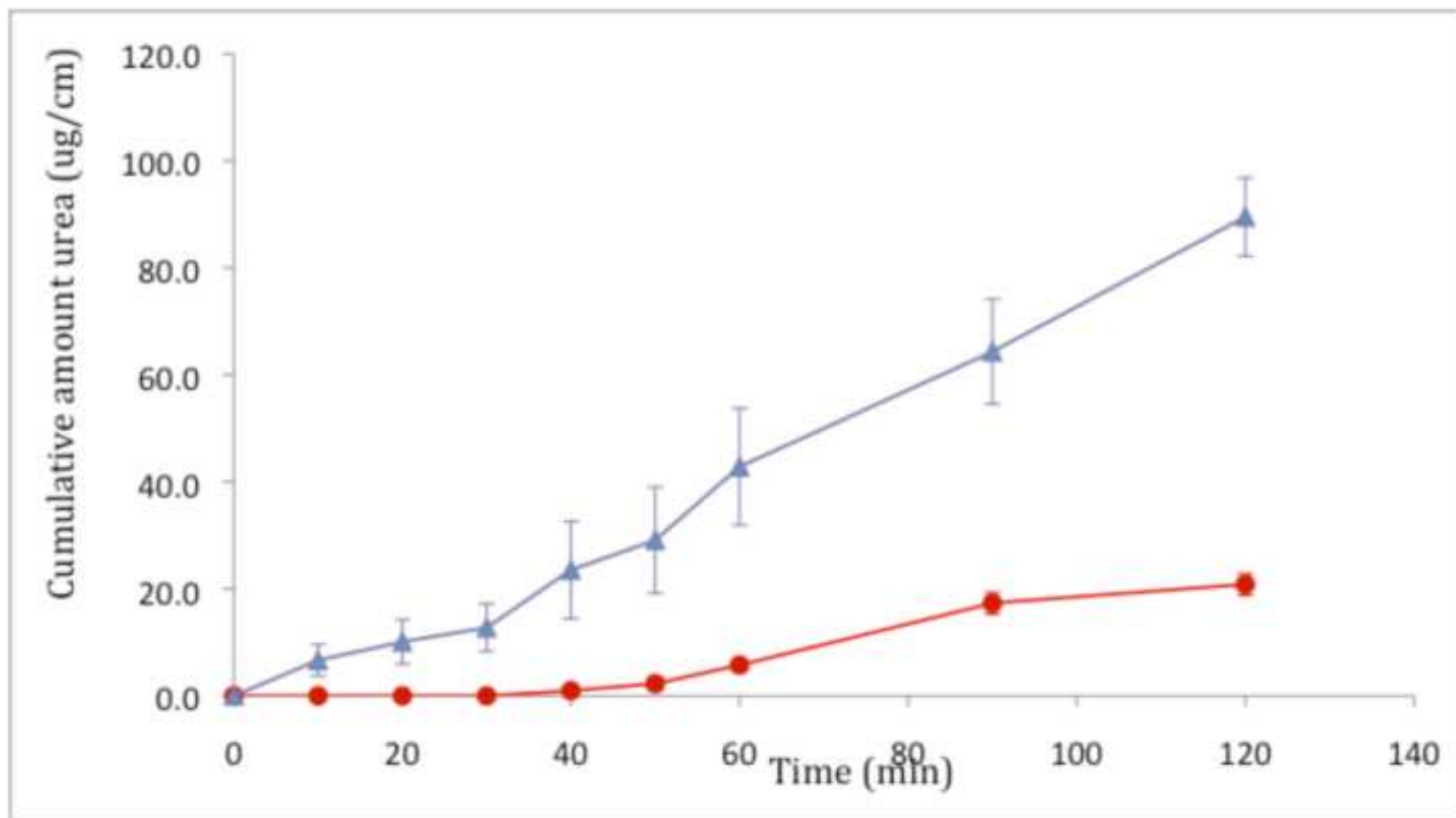


Figure 4  
[Click here to download high resolution image](#)

